J. Phys. Chem. Solids Vol. 53, No. 5, pp. 681–685, 1992
Printed in Great Britain.

0022-3697/92 $5.00 + 0.00

STUDIES ON THE MECHANISM OF THERMAL DEHYDRATION OF COBALT OXALATE DIHYDRATE

A. VENKATARAMAN,† N. V. SASTRY and ARABINDA RAY
Department of Chemistry, Sardar Patel University, Vallabh Vidyanagar 388 120, Gujarat, India

(*Received* 4 *February* 1991; *accepted* 9 *October* 1991)

Abstract—Several mechanistic and non-mechanistic equations are employed to compute kinetic parameters from TG studies of cobalt oxalate dihydrate. A phase boundary reaction mechanism is suggested for the dehydration step. Spectroscopic, magnetic and elemental micro-analysis results supplement the mechanism as proposed by TG analysis. A DSC trace also supports the mechanism.

Keywords: Mechanism, thermal dehydration, TG studies, spectroscopic data.

1. INTRODUCTION

The dehydration and decomposition of transition metal oxalates are well documented in the literature. Dollimore [1] has reviewed extensively the thermal decomposition and dehydration of metal oxalates along with their useful analytical applications. Smith and Topley [2] found that the mechanism of dehydration of manganese oxalate dihydrate depends on the vapour pressure of water vapour above the sample. Fong and Chen [3, 4] have evaluated the kinetic parameters for thermal dehydration of $Mg(OH)_2$. Krishnan and Ninan [5] reported on the dehydration of zinc oxalate dihydrate from TG data. Both these studies employed several mechanistic equations to treat the thermal data and aimed at proposing the mechanism of dehydroxylation and dehydration. It appears, however, that spectroscopic data have been inadequately used to study the structural aspects of the mechanism of dehydration.

This communication deals with studies on the dehydration mechanism of cobalt oxalate dihydrate using mainly thermal data, supplemented by spectroscopic (i.r., vis reflectance) studies, magnetic measurements and micro-elemental analysis results. It is hoped that the spectral studies of both hydrated and dehydrated cobalt oxalate would help in better understanding the mechanism of dehydration.

2. EXPERIMENTAL

2.1. *Material*

Cobalt oxalate dihydrate ($CoC_2O_4 \cdot 2H_2O$) was prepared by mixing equimolar solutions of cobalt sulfate heptahydrate and oxalic acid dihydrate under dynamic nitrogen atmosphere at room temperature with through shaking. The chemicals used were of B.D.H. Analar grade.

The dehydration of the sample was carried out in a specially-built furnace in static air at a temperature of 208°C for 30 min and dried in vacuum before taking the measurements.

Anal. Calcd. for $CoC_2O_4 \cdot 2H_2O$:C 13.12%; H 2.2%;
Found C 13.68%; H 2.504%;
Calcd. for CoC_2O_4:C 16.33%;
Found C 16.60%.

2.2. *Physico-chemical measurements*

I.R. spectra were recorded on a Perkin Elmer 983 infrared spectrophotometer in the 4000–180 cm^{-1} range using KBr pellets. A Beckman DK-2A spectrophotometer was employed to obtain visible reflectance spectra of the samples. Magnetic susceptibility of the samples was obtained using a Gouy balance. A Colmen C–H–N analyser was used for C and H determinations.

TG measurements were carried out with a Du Pont 951 thermogravimetric analyser under static air atmosphere using different heating rates and sample masses. A DSC trace was obtained using a Du Pont Differential Scanning Calorimeter 910 under dynamic nitrogen atmosphere.

X-ray diffraction studies of powder samples of cobalt oxalate dihydrate and dehydrated cobalt oxalate were obtained using a Philips PW 1130 X-ray diffractometer with CoK_α target.

All computations were made using the HCl 80386 computer at the Department of Chemistry.

3. MATHEMATICAL TREATMENT OF DATA

The kinetic parameters were evaluated from the mechanistic equations in the Coats and Redfern

---

†Author to whom correspondence should be addressed.

Table 1. Commonly used $g(\alpha)$ forms of solid state reactions

Eqn No.	Forms of $g(\alpha)$	Rate controlling process
(1)	α^2	One-dimensional diffusion
(2)	$\alpha + (1-\alpha)\ln(1-\alpha)$	Two-dimensional diffusion
(3)	$[1-(1-\alpha)^{1/3}]^2$	Three-dimensional diffusion spherical symmetry, Jander equation
(4)	$[1-(2/3)\,\alpha]-[1-\alpha]^{2/3}$	Three-dimensional diffusion, spherical symmetry, consisting Brounshtein equation
(5)	$-\ln(1-\alpha)$	Ramdom nucleation, one nucleus on each particle, Mamphel equation
(6)	$[-\ln(1-\alpha)]^{1/2}$	Random nucleation, Avrami eqn I
(7)	$[-\ln(1-\alpha)]^{1/3}$	Random nucleation, Avrami eqn II
(8)	$1-(1-\alpha)^{1/2}$	Phase boundary reaction, cylindcrical symmetry
(9)	$1-(1-\alpha)^{1/3}$	Phase boundary reaction, spherical symmetry
(10)	$1-(1-\alpha)^n,\ n=1$	Reaction order
(11)	$1-(1-\alpha)^n,\ n=2$	Reaction order
(12)	$1-(1-\alpha)^n,\ n=3$	Reaction order
(13)	$1-(1-\alpha)^n,\ n=4$	Reaction order

form to evaluate the possible rate controlling process, as suggested by Satava [6] and Gallagher *et al.* [7]. The general form of the equation used is

$$\ln\left(\frac{g(\alpha)}{T^2}\right)=\ln\left(\frac{AR}{\phi E_a}\right)-\left(\frac{E_a}{RT}\right). \qquad (1)$$

The commonly used $g(\alpha)$ forms for solid state reaction along with the rate controlling processes are given in Table 1.

Along with these mechanistic equations four other non-mechanistic methods suggested by Coats and Redfern [8] (C–R), Borido [9], Horowitz and Metzger [10] (H–M) and Freeman and Carroll [11] (F–C) are used for comparison.

Using a computer the differential form $d\alpha/dT$ was evaluated by a regression equation of the form

$$\alpha = a_1 + a_2T + a_3T^2.$$

The following values of the coefficients $a_1 = -10.5$, $a_2 = +0.04095$ and $a_3 = 0.000039$, were obtained.

The TG data were treated by a linear least square computer program to evaluate the kinetic parameters viz. activation energy E_a, frequency factor A and the correlation coefficient r.

4. RESULTS AND DISCUSSION

4.1. *Vibrational modes*

Raman and i.r. studies of free oxalic acid assigned a C_{2h} point group symmetry to this molecule [12]. A strong Raman band at 1760 cm^{-1} has been attributed to sym C=O stretching. The asym C=O stretching appears at 1650 cm^{-1} in the infrared [12].

The i.r. spectrum (Table 2) of the cobalt oxalate dihydrate complex, however, shows a strong absorption around 1700 cm^{-1}. This probably suggests bonding of the C=O moiety to the metal. Because of this complexing the symmetry of this oxalic moiety has changed and the 1760 cm^{-1} Raman band of the free acid appeared at 1700 cm^{-1} in the complex. The 1700–1550 cm^{-1} region is very broad in the cobalt oxalate dihydrate complex and therefore the bending mode of coordinated H_2O could not be assigned.

The dehydrated cobalt oxalate complex, however, has only an intense peak around 1600 cm^{-1} (Table 2). This band can be assigned only to C=O stretching. Such a steep decrease in the C=O stretching mode is not unexpected considering the fact that removal of coordinated water has made the Co–O bond stronger.

By comparison with comparable molecules [13] the absorptions at 1400 and 1360 cm^{-1} in cobalt oxalate. $2H_2O$ are assigned to coupled vibrations of $\nu_{C\text{-}O}$ and

Table 2. Important i.r. bands on $CoC_2O_4 \cdot 2H_2O$ and dihydrated $CoC_2O_4 \cdot 2H_2O$ complexes

Compound	i.r. bands (cm^{-1})	Compound	i.r. bands (cm^{-1})	Assigned
$CoC_2O_4 \cdot 2H_2O$	1700	CoC_2O_4	1600	$\nu_{C=O}$
	1400		1370	$\nu_{C\text{-}O} + \nu_{CC}$
	1360		1320	$\nu_{C\text{-}O} + \nu_{CC}$
	760		—	ρCo–OH$_2$ (rock)
	670		—	ωCo–OH$_2$ (wag)
	440		—	$\nu_{Co\text{-}OH_2}$
			560	$\nu_{Co\text{-}O} + \nu_{C\text{-}C}$
			470	$\nu_{Co\text{-}C}$ + ring defor

$\nu_{C\text{-}C}$ modes (Table 2). These absorptions are shifted to 1370 and 1320 cm^{-1} in the i.r. spectrum of the dehydrated complex. These shifts may be attributed to the stronger Co–O bond in the dehydrated cobalt oxalate complex.

The Co–OH_2 rocking, wagging and stretching modes are assigned to 760, 670 and 440 cm^{-1}, respectively (Table 2) in the Co(II) oxalate dihydrate. These compare well with the values reported for similar compounds [14]. As expected these peaks are absent in the dehydrated form.

The Co–O stretching for dehydrated Co(II) oxalate complex is distributed in the frequencies at 560 and 470 cm^{-1} (Table 2). The said mode, however, could not be identified in the cobalt oxalate dihydrate complex as the region 660–450 cm^{-1} is practically a featureless broad absorption in the compound.

4.2. *Electronic spectra and magnetic moment*

The electronic spectrum (reflectance) of $CoC_2O_4 \cdot 2H_2O$ complex has the appearance of a typical octahedral complex. The band around 20,000 cm^{-1} is accordingly assigned to $^4T_{1g}(F) \rightarrow {}^4T_{1g}(P)$. The shoulder at 22,220 cm^{-1} may be due to spin–orbit coupling [15]. The very weak band at 16,660 cm^{-1} in the present investigation may be assigned to the $^4T_{1g}(F) \rightarrow {}^4A_{2g}$ transition [14].

The magnetic moment value of 5.2 B.M. for this complex agrees well with that for octahedral complexes of Co(II) [16].

Since the electronic spectrum was obtained in the solid state, the absorption coefficients could not be employed to add to the determination of the geometry of the dehydrated Co(II) complex. However, it appears that the data might fit a tetrahedral geometry around the Co(II) ion in the complex [17]. The main peak at 19,000 cm^{-1} may be assigned to a $^4A_1 \rightarrow {}^4T_1(P)$ transition. The actual symmetry in a dehydrated Co(II) complex may not be exactly tetrahedral, but nearer to C_{2v}. This will cause splitting [18] and might be the reason for a number of shoulders at 22,000, 20,000 and 17,860 cm^{-1}.

The magnetic moment value of 4.75 B.M. corresponds to a tetrahedral geometry [15] of the dehydrated complex.

4.3. *Structure of the complexes*

The elemental analysis, spectroscopic and magnetic moment data suggest the structure of Fig. 1 for cobalt oxalate dihydrate complex. The polymeric structure is necessary to satisfy the six coordination of Co(II). The TG data have also confirmed the presence of coordinated water. For each Co(II) ion one water molecule is above and one below the plane containing the oxalate moiety.

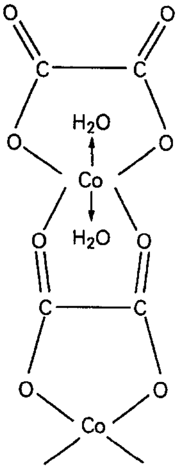

Fig. 1. Structure of cobalt oxalate dihydrate.

For the dehydrated Co(II) oxalate complex, a polymeric structure similar to the hydrated one may be proposed, the difference being the presence of tetrahedral/pseudo tetrahedral Co(II) in the former.

4.4. *Thermal analysis*

A typical TG curve for cobalt oxalate dihydrate is shown in Fig. 2. It shows two distinct steps and the first step corresponds to the loss of two water molecules from the parent compound. The second step is attributed to the decomposition of dehydrated cobalt oxalate to cobalt oxide (Co_3O_4). The dehydration step is initiated at 157.5°C and is completed at 212.5°C, the usual range representing the loss of coordinated water in similar compounds. The decomposition step started at 337.5°C and was completed at 370°C.

The kinetic parameters viz. the activation energy E_a and frequency factor A were calculated for the dehydration step by employing several mechanistic and non-mechanistic equations to elucidate the mechanism of dehydration. Table 3 presents the kinetic parameters as calculated from different mechanistic equations. The E_a values varied from 8 $kcal mol^{-1}$ to 54 $kcal mol^{-1}$ and the order of A value ranged from 10^1 to 10^{25}. The significance of these results can only be appreciated by comparing the kinetic parameters calculated from the C–R equation, which gives one of the best solutions for such studies and also represents a general form for all the different mechanistic equations. Table 4 gives the values for E_a and A for different non-mechanistic equations. A comparison of E_a and A values of Tables 3 and 4 shows that mechanistic eqns (5), (8) and (9) give similar values to those of the C–R equation.

As for the correlation coefficient, value (r), the mechanism of dehydration is supposed to follow eqns

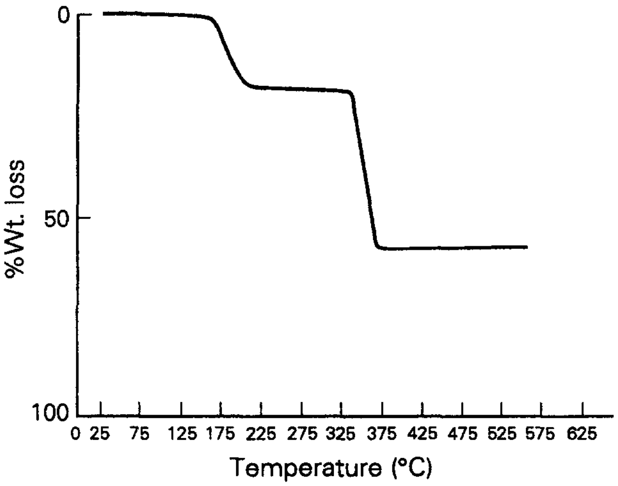

Fig. 2. TG trace of cobalt oxalate dihydrate (in air).

(8) and (9). The order *n* of the dehydration of cobalt oxalate dihydrate was presumed to be 1.0 but the *n* value derived from the F–C method was found to be −0.0125, though the *r* value was 0.962. This discrepancy prompted us to perform curve-fitting analysis by using a computer programme entitled CURVEFT (version 2.10 K by Thomas S. Cox published by IMTEC Box 1402, Bowie, MD 20716, U.S.A.). The software is capable of handling 25 different forms of least square fittings. Our data were found to give a best fit with $r = 0.982$ in a non-linear form of the type

$$Y=\left(\frac{X}{AX+B}\right),$$

where

$$Y=\frac{\ln(d\alpha/dT)}{\ln(1-\alpha)} \quad \text{and} \quad X=\frac{(1/T)}{\ln(1-\alpha)}.$$

Looking into this, it can be reasonably and cautiously stated that the kinetic parameters cannot be evaluated by using the F–C equation.

Table 3. Kinetic parameters calculated on the basis of mechanistic equations for thermal dehydration of $CoC_2O_4 \cdot 2H_2O$ from TG curves: heating rate = 10°C min^{-1}; atmosphere = static air. Sample mass = 7.94 mg

Equation numbers according to Table 1	Activation energy E_a (kcalmol^{-1})	Frequency factor A
(1)	43.106	3.67×10^{18}
(2)	44.403	8.125×10^{18}
(3)	44.963	3.544×10^{18}
(4)	10.921	9.448×10^{18}
(5)	21.990 (0.960)	1.717×10^{9}
(6)	9.960	4.39×10^{3}
(7)	9.056	5.313×10^{1}
(8)	21.398 (0.990)	4.22×10^{8}
(9)	21.517 (0.990)	3.25×10^{8}
(10)	17.511	1.71×10^{7}
(11)	11.694	2.00×10^{2}
(12)	17.143	1.667×10^{7}
(13)	54.721	2.499×10^{25}

Values in parentheses show correlation coefficient, *r*.

The similarity of the E_a and A values of the C–R equation and eqns (8) and (9) of Table 3 leads to significant ideas about the possible and probable mechanism of water loss from the parent compound. Equations (8) and (9) propose simultaneously cylindrical and spherically symmetrical phase boundary reactions. Therefore, the following mechanism is contemplated for this dehydration study. The coordinated water molecules are thought to reach the phase boundary by diffusion both in a spherical and cylindrical manner, resulting in a pseudo-tetrahedral configuration of dehydrated cobalt oxalate, as observed from spectral and magnetic studies.

The mechanism of dehydration was found to be independent of the mass of sample and heating rate.

Table 4. Kinetic parameters calculated on the basis of non-mechanistic equations for thermal dehydration of $CoC_2O_4 \cdot 2H_2O$ from TG curve: heating rate: 10°Cmin^{-1}; atmosphere: static air; sample mass: 7.94 mg

Name of the equation	Activation energy E_a (kcalmol^{-1})	Frequency factor A
C–R relation	21.920 (0.999)	7.47×10^{8}
Broido relation	41.553	9.11×10^{24}
H–M relation	18.798×10^{5}	—
F–C relation	8.304 (0.962)	−0.0125†

† Show order of the reaction; values in parentheses show correlation coefficient, *r*.

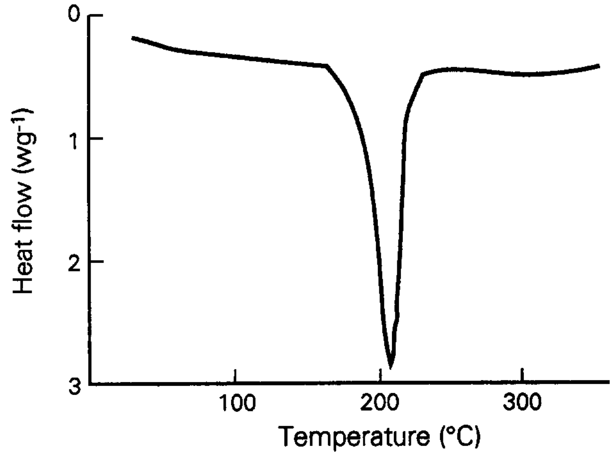

Fig. 3. DSC trace of cobalt oxalate dihydrate (in N_2 atmosphere).

Figure 3 represents the DSC curve for a cobalt oxalate dihydrate sample showing a sharp endothermic peak corresponding to the dehydration process. The peak temperature was 183.87°C. The heat of dehydration, ΔH, and heat capacity, C_p, values were computed from the DSC curve. The C_p value was found to be 7.982 calg^{-1}°C, which is higher than the reported value of 4.397 calg^{-1}°C for water formation from the pure components [19]. The C_p value for this reaction corresponds to the energy for rupture of Co–OH_2 bonds and the energy changes involved for shifting the symmetry of the complex to tetrahedral/pseudotetrahedral.

4.5. *X-ray diffraction* (*XRD*) *studies*

Cobalt oxalate dihydrate has been reported to exist in α- and β-forms [20, 21]. The XRD pattern (Table 5) of the cobalt oxalate dihydrate prepared in this laboratory agrees well with the β-form [21]. The XRD pattern (Table 5) of the dehydrated cobalt oxalate shows only a few prominent peaks and probably indicates the loss of crystallinity.

Table 5. XRD data of $CoC_2O_4 \cdot 2H_2O$ and CoC_2O_4

Observed *d*-spacing values† of $CoC_2O_4 \cdot 2H_2O$ in present study	Observed *d*-spacing values† of CoC_2O_4 in present study
4.720 (vs)	4.72 (vs)
3.880 (m)	3.89 (s)
3.560 (m)	3.68 (s)
2.940 (s)	
2.638 (m)	
2.563 (m)	
2.360 (w)	
2.230 (m)	
2.150 (w)	
2.085 (w)	
2.020 (m)	
1.985 (w)	
1.918 (w)	
1.895 (w)	
1.877 (w)	
1.791 (w)	

† vs indicates very strong; s indicates strong, m indicates medium and w indicates weak intensity peaks, respectively.

Acknowledgements—One of the authors, AVR, would like to thank the U.G.C., New Delhi, for financial help. The encouragement rendered by Prof. V. S. Patel, Head, Department of Chemistry, is gratefully acknowledged.

REFERENCES

1. Dollimore D., *Thermochimica Acta* **117,** 331 (1987).
2. Topley F. B. and Smith M. L., *J.C.S.* **321,** (1935).
3. Pong H. F. and Chen D. T. Y., *Thermochimica Acta* **17,** 000 (1976).
4. Pong H. F. and Chen D. T. Y., *ibid.* **18,** 273 (1977).
5. Krishnan K. and Ninan K. N., *ibid.* **89,** 295 (1985).
6. Satava V., *ibid.* **2,** 2 (1971).
7. Gallagher P. K. and Johnson D. W., *ibid.* **6,** 67 (1973).
8. Coats A. W. and Redfern J. P., Nature (London) **201,** 69 (1964).
9. Brodio A. J., *Poly. Sci.* **A-27,** 1761 (1969).
10. Horwitz H. H. and Metzger G., *Anal. Chem.* **35,** 1464 (1963).
11. Freeman E. S. and Carroll B., *J. Phys. Chem.* **62,** 394 (1958).
12. Murata H. and Kwai K., *J. Chem. Phys.* **25,** 589 (1956).
13. Fujita J., Martell A. E. and Nakamoto K., *J. Chem. Phys.* **36,** 324, 331 (1962).
14. Nakagawa I. and Shimanouchi T., *Spectrochim. Acta* **20,** 429 (1964).
15. Lever A. P. B., *Inorganic Electronic Spectroscopy.* Elsevier, New York (1984).
16. Cartin R. L., *Transition Metal Chemistry* (Edited by R. Carlin), Vol. 1, pp. 1–31. Marcel Dekker, New York (1965).
17. Simo C. and Holt S., *J. Inorg. Chem.* **7,** 2655 (1968).
18. Sexana A. and Jha N. K., *Inorg. Nucl. Chem.* **40,** 1601 (1978).
19. *International Critical Tables,* Vol. VII, p. 232. McGraw-Hill, New York (1930).
20. ASTM file index 25–251.
21. ASTM file index 25–250.